Phenol Formaldehyde Resin Nanoparticles Loaded with CdTe Quantum Dots: A Fluorescence Resonance Energy Transfer Probe for Optical Visual Detection of Copper(II) Ions

Ping Yang,[†,‡] Yang Zhao,[†] Yang Lu,[†] Qi-Zhi Xu,[†] Xue-Wei Xu,[†] Liang Dong,[†] and Shu-Hong Yu[†,*]

[†]Division of Nanomaterials and Chemistry, Hefei National Laboratory for Physical Sciences at Microscale, Department of Chemistry, the National Synchrotron Radiation Laboratory, University of Science and Technology of China, Hefei, Anhui 230026, P. R. China, and [‡]Department of Chemistry and Chemical Engineering, Huainan Normal University, Huainan, Anhui 232001, P. R. China

ABSTRACT A novel fluorescence resonance energy transfer (FRET) system has been designed for the Cu^{2+} ions detection with optical visual assays. In this FRET reaction, the biocompatible, green luminescent monodisperse phenol formaldehyde resin nanoparticles (PFR NPs) synthesized by a simple hydrothermal method were used as the acceptor and the luminescent CdTe quantum dots (QDs) were selected as the donor. By the layer-by-layer method, the polyelectrolyte (PEI/PSS/PEI) were absorbed alternately on the surface of the PFR NPs. As a result, the amino groups were stably modified onto the surface of the PFR NPs. In the presence of 1-ethyl-3-(3-dimethly aminopropyl) carbodiimide (EDAC) and *N*-hydroxysuccinimide (NHS), the carboxyl groups coated CdTe QDs prepared by using mereaptoactetic acid (MA) as the stabilizer in water solution were coupled to the surface of amino group functionalized PFR NPs to obtain novel FRET nanocomposites. Owing to the sensitive quenching effect of Cu^{2+} ions on CdTe QDs and effective energy transfer from CdTe QDs to PFR NPs, the as-prepared FRET nanocomposites were utilized to monitor Cu^{2+} ion with optical visual detection at room temperature within 1 min. This nanoparticle-based FRET probe should promote further development of other nanocomposites for Cu^{2+} ion detection in the environmental field.

KEYWORDS: fluorescence resonance energy transfer (FRET) · phenol formaldehyde resin (PFR) nanoparticles · CdTe quantum dots · optical visual detection · copper(II) ions

To improve the sensitivity of the fluorescence probe, fluorescence resonance energy transfer (FRET) has been widely used as an extremely useful tool in bioanalytical and biosensing applications.[1−4] In a FRET process, the excitation light is absorbed by the donor first, and then the energy is transferred from the donor to the acceptor luminophor *via* a nonradiative multipole coupling mechanism.[5] The FRET occurs only when their emission and absorption bands overlap sufficiently and their mutual distance is close enough.[6] Recently, the FRET systems have been introduced into quantum dot (QD)-based luminescence analysis for protein[7−9] and detection of other environmental samples.[10−14] However, just a few of the FRET biosensors have involved QD donors and functionalized Au nanoparticle (NP) acceptors in biological detection and chemical analysis.[15−18] Therefore, to synthesize the novel nanoparticles with good biocompatibility and excellent luminescence similar to the FRET acceptor is of importance in biotechnology and material science. Recently, our group has reported the synthesis of biocompatible, green luminescent monodisperse phenol formaldehyde resin (PFR) NPs with controllable size by a facile one-step hydrothermal method.[19] The as-synthesized PFR NPs have a noticeable absorption at 610 nm, which makes it an appropriate energy acceptor in a FRET system. Thus, it is desirable to design a novel FRET probe where the size of CdTe QDs donor is adjusted to well match that of the PFR NPs acceptor.

As an essential trace element for organisms, besides iron and zinc, copper is one of the most abundant transition metal ions in the human body. However, it also brings serious environmental contamination and potential toxicity to living organisms.[20,21] Various sensor systems have been developed for the detection of copper ions at trace quantity levels in various samples, such as the fluorescence method based on luminescent nanomaterials,[22−24] atomic absorption spectroscopy,[25,26] inductively couple

* Address correspondence to shyu@ustc.edu.cn.

Received for review December 7, 2010 and accepted January 28, 2011.

Published online February 23, 2011
10.1021/nn103352b

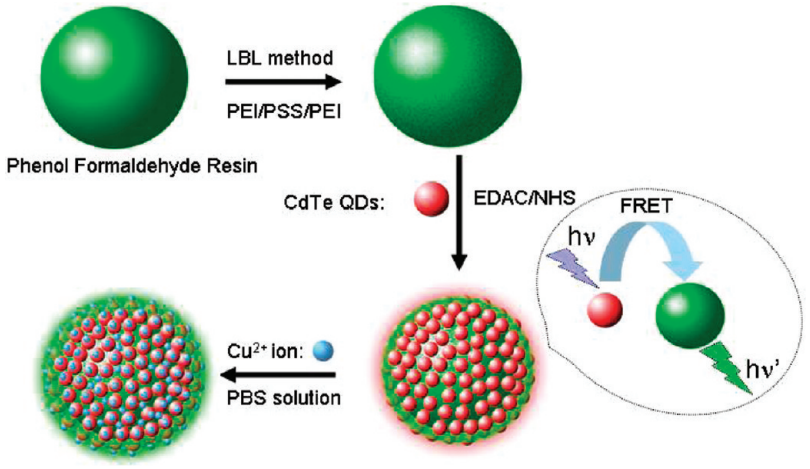

Scheme 1. Schematic illustration of the synthesis of the PFR-CdTe QDs FRET probe and the optical color change induced by Cu^{2+} ions.

plasma mass spectroscopy (ICPMS),[27] inductively coupled plasma atomic emission spectrometry (ICP—AES),[28] absorbance spectro-photometry,[29] and voltammetry.[30,31] In recent years, an optical visual method has been a growing focus for metal ions such as calcium(II) ion,[32,33] lead(II) ion,[34,35] mercury(II) ion,[36−39] and other substances[40−42] due to easily being read with the naked eye. Most of these protocols need a polymeric aggregate of DNA-functionalized gold nanoparticles with DNA duplex interconnects. Nevertheless, a sensitive sensing Cu^{2+} ion with visual detection methods has rarely been reported.[43−46] Some of these methods are based upon the aggregation of gold nanoparticles functionalized by DNAzyme or organic compounds, and the sensitive detection limit can meet the requirement for environmental sample assay. Thus, to find a more appropriate and easier method for Cu^{2+} visual detection remains a big challenge.

Herein, to combine the advantage of the excellent fluorescence features of the CdTe QDs and the biocompatible, green luminescent monodisperse PFR NPs, a novel FRET system has been designed using about 4.1 nm CdTe QDs as the donor and green luminescent PFR NPs as the acceptor. Furthermore, the FRET probe was utilized to monitor Cu^{2+} with optical visual detection at room temperature within 1 min.

RESULTS AND DISCUSSION

As shown in Scheme 1, the FRET probe consists of two parts. First, the $-NH_2$ groups were introduced onto the surface of PFR NPs with a size of about 300 nm using poly(sodium 4-styrene-sulfonate) (PSS) and polyethylenimine (PEI) by layer-by-layer method (Scheme 1). The hydrodynamic diameters of PFR NPs in aqueous solution were determined by dynamic light scattering (DLS) analysis (see Supporting Information Figure S1). Because of rich hydroxyl on the surface of PFR, the corresponding hydrodynamic diameters of nanoparticles were larger than the particles observed in TEM images. The process of functionalizing PFR with polyelectrolyte was monitored by the zeta potential analysis. The surface charge of the naked PFR NPs is weak positively charged (5.0 mV) in water (see Supporting Information Figure S2). With the alternating absorption of the polyelectrolyte (PEI/PSS/PEI), the zeta potential of the nanocomposites alternated from negative to positive values, which implied that PSS and PEI were absorbed alternately onto the surface of PFR NPs. As a result, the amino groups were stably modified onto the surface of the PFR NPs. Second, the carboxyl groups coated CdTe QDs prepared by using mereaptoactetic acid (MA) as the stabilizer in water solution[47] were coupled to the surface of amino group functionalized PFR NPs in the presence of 1-ethyl-3-(3-dimethly aminopropyl) carbodiimide (EDAC) and *N*-hydroxysuccinimide (NHS). The FTIR spectra of the PFR and the PFR—QD nanocomposites were shown in Supporting Information Figure S3. The bands in the range of 1637—755 cm^{-1} are consistent with those of the pure PFR.[48] However, the band at 1579 cm^{-1} is assigned to the coupling reaction of δ_{NH} and δ_{C-N} of the carbonyl group II band, which indicated that CdTe QDs were coupled with the PFR NPs successfully. The XPS spectrum further identifies the results described above (see Supporting Information Figure S4). The peak deconvolution of C(1s) at 288.3 eV (curve c) demonstrates the existence of the carbonyl group, suggesting that the CdTe QDs were conjugated onto the surface of PFR. The transmission electron microscopy (TEM) image of the prepared CdTe QDs-PFR nanocomposites directly indicates the formation of the multicomponent nanospheres (Figure 1).

The fluorescent property of the novel FRET probe prepared by the CdTe QDs and PFR NPs was studied in detail. As it has been reported, the PFR NPs have a strong absorption peak at about 610 nm. In the meantime, it also can emit green visible luminescence at 520 nm (Figure 2A, curve a),[19] while the 4.1 nm CdTe QDs possess a strong

emission at 608 nm (Figure 2A, curve b). When 188 μmol/L as-prepared CdTe QDs (Figure 2B, curve b) were coupled to the surface of PFR NPs (0.1 mg/mL) (Figure 2B, curve a), the FRET occurred (Figure 2B, curve c) and the luminescence of PFR NPs (acceptor) doubly enhanced due to the energy transfer from the CdTe QDs. Meanwhile, the fluorescence intensity of the QDs (donor) decreased and the emission wavelength at 608 nm had about 10 nm red-shift. However, the whole solution was observed to emit red light under UV light (365 nm) excitation because the eyes are more sensitive to red than green. Figure 2C shows that the CdTe QDs at appropriate concentration (94−188 μmol/L) can transfer the energy to PFR NPs effectively, resulting in noticeable enhancement of the luminescence of PFR NPs (Figure 2C, curves a, b). Additional CdTe QDs (292 μmol/L) cannot offer more energy for PFR NPs (Figure 2C, curve c) assigned to the fluorescence self-quenching of high concentration of CdTe QDs, even if the red light was observed more obviously (Figure 2C, inset). In the meantime, the effect of various concentrations of PFR (curve a, 0.1; curve b, 0.3; curve c, 0.5; curve d, 1 mg/mL) on the luminescence of PFR−QDs nanocomposites in the presence of 292 μmol/L CdTe QDs was investigated. Figure 2D shows that 0.5 mg/mL PFR (curve c) can obtain enough energy from the QDs, so 0.5 mg/mL PFR and 188 μmol/L CdTe QDs were used for the preparation of PFR−QDs nanocomposites in this experiment.

To explore the practicability of the novel FRET probe based upon PFR−QDs nanocomposites, it was used to detect Cu^{2+} by an optical visual method. As previously described, Cu^{2+} was considered to be particularly useful for inhibiting the emission of CdSe/CdTe QDs under the cooperation of the thiol group on the surface of the QDs and the cadmium ions in the QDs.[25] Therefore, we propose that the efficiency of FRET between PFR and QDs would be influenced in the presence of Cu^{2+} ions, leading to a noticeable PL change of the PFR−QDs nanocomposites under UV excitation. As a consequence, the concentration of Cu^{2+} could be directly reflected by the color change of nanocomposites and thus the PFR−QDs probe may be an ideal optical colorimetric sensor for Cu^{2+} detection.

As shown in Figure 3A, the intensity of QDs in the PFR−CdTe QDs nanocomposites was quenched selectively and effectively by 1 μmol/L copper ions which was minimally affected by other cations. Correspondingly, no remarkable optical color change of the solution was observed in the presence of these selected metal ions, only the solution containing of copper ions became green in Figure 3B. The specific detection for

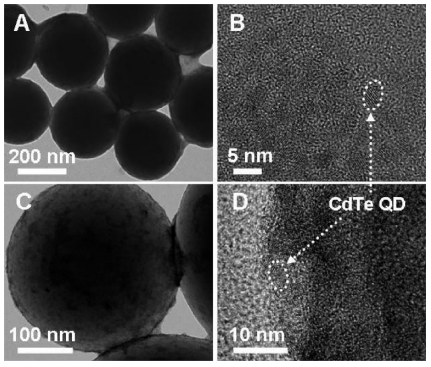

Figure 1. TEM and HRTEM images of the as-prepared PFR−QDs nanocomposites (A, C, D) and the CdTe QDs (B).

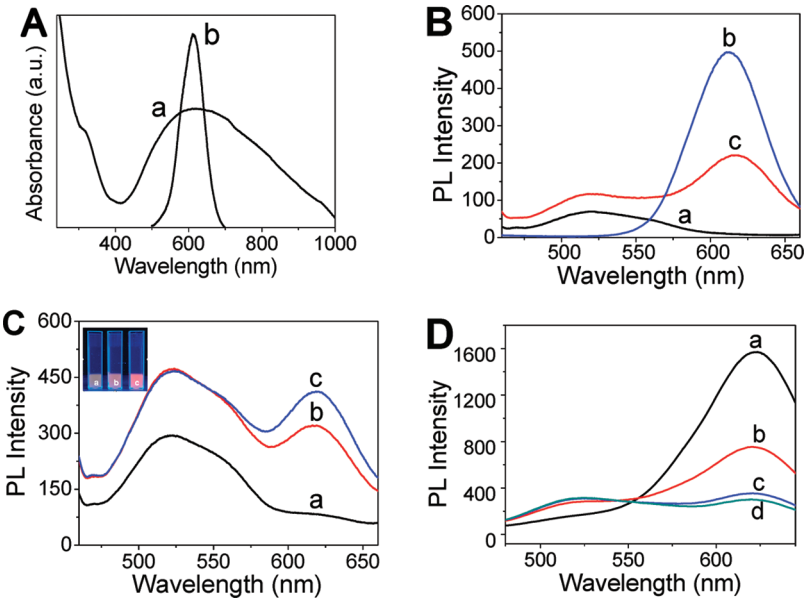

Figure 2. (A) The absorbance spectrum of PFR (curve a) and the PL spectrum of QDs (curve b); (B) The PL spectrum of the FRET (curve c) between 0.1 mg/mL PFR NPs (curve a) and 188 μmol/L CdTe QDs (curve b); (C) The PL spectra of FRET nanocomposites composed of different concentrations of CdTe QDs (a, 94; b,188; c, 292 μmol/L) and 0.5 mg/mL PFR NPs ; (D) The PL spectra of FRET probe composed of different concentrations of PFR NPs (a, 0.1; b, 0.3; c, 0.5; d, 1 mg/mL) and 292 μmol/L QDs.

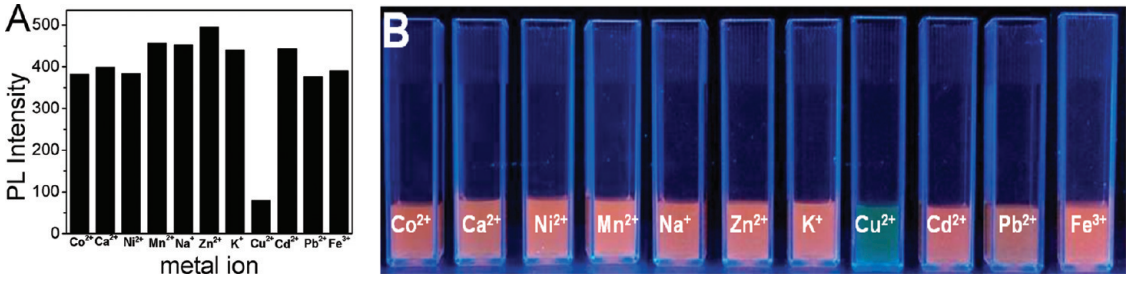

Figure 3. (A) Effect of different ions (Co^{2+}, Ca^{2+}, Ni^{2+}, Mn^{2+}, Na^{+}, Zn^{2+}, K^{+}, Cu^{2+}, Cd^{2+}, Pb^{2+} and Fe^{3+} with the concentration of 1 μmol/L, respectively) on the luminescence intensity of QDs in the 0.5 mg/mL PFR-CdTe QDs nanocomposites; (B) Optical color response of the FRET system based on 0.5 mg/mL PFR−QDs nanocomposites in the presence of a series of selected metal ions (Co^{2+}, Ca^{2+}, Ni^{2+}, Mn^{2+}, Na^{+}, Zn^{2+}, K^{+}, Cu^{2+}, Cd^{2+}, Pb^{2+}, Fe^{3+} with concentrations of 10, 100, 10, 10, 100, 100, 100, 3.5, 10, 10, 5 μmol/L, respectively) in PBS solution (pH 7).

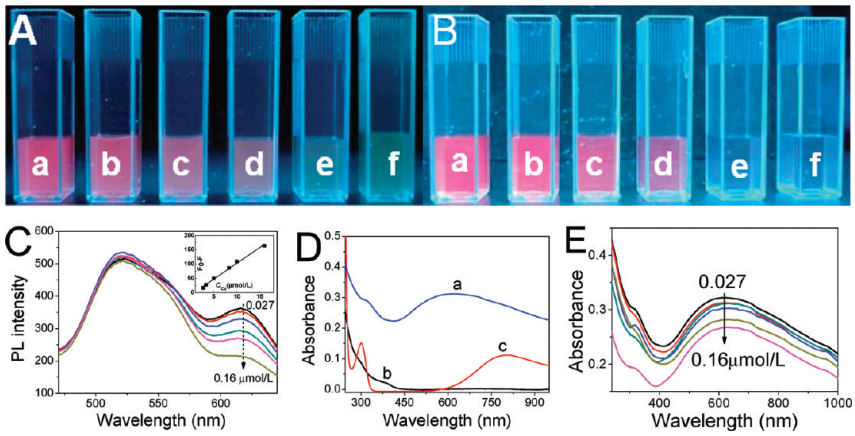

Figure 4. (A) The photographs showing the influence of the concentration of Cu^{2+} ions (0.08, 0.16, 0.25, 0.43, 2.87, and 5.36 μmol/L) on the fluorescence color change of the 0.5 mg/mL PFR−CdTe QDs FRET probe in PBS solution (pH 7); (B) The photographs showing the influence of the concentration of Cu^{2+} ions (0.08, 0.16, 0.25, 0.43, 2.87, and 5.36 μmol/L) on the fluorescence color change of the pure 188 μmol/L CdTe QDs in PBS solution (pH 7); (C) The PL spectra of 0.5 mg/mL PFR−QDs probe in the presence of different concentration of Cu^{2+} ions (from 0.027 to 0.16 μmol/L) in PBS solution (pH 7); (D) The absorbance of 0.5 mg/mL PFR NPs (curve a), 188 μmol/L CdTe QDs (curve b), and Cu^{2+} ion (curve c); (E) The absorption spectra of 0.5 mg/mL PFR−QDs probe in the presence of various concentrations of Cu^{2+} ions (from 0.027 to 0.16 μmol/L) in PBS solution (pH 7).

Cu^{2+} ions is clearly attributed to its sensitivity to the luminescence of QDs.

The sensitivity experiment of the novel FRET probe was investigated in the presence of different concentrations of Cu^{2+} ions. As anticipated, upon addition of various concentrations (0.08, 0.16, 0.25, 0.43, 2.87, and 5.36 μmol/L) of Cu^{2+} ions in the system, the red color of mixture changed into green gradually (Figure 4A). Compared with pure QDs (Figure 4B) in the presence of the same concentration of copper ions, the FRET probe exhibits more sensitivity for visual detection of Cu^{2+} ions. Figure 4A shows that the optical color was sensitive for Cu^{2+} ions from 0.08 to 5.36 μmol/L. Under the same conditions, when QDs were exploited for the visual detection of Cu^{2+} ions, the range of the optical color change was only from 0.16 to 2.87 μmol/L (Figure 4B). In the presence of FRET probe, the minimum concentration of Cu^{2+} ions for resulting in distinct optical color change of the system was 0.16 μmol/L. However, only when the concentration of Cu^{2+} ions went to 0.25 μmol/L, the optical color of QDs changed. There are two reasons for this phenomena. First, due to the energy transfer from CdTe QDs to PFR NPs, the PL intensity of PFR increases and the green luminescence of PFR in the FRET system is more sensitive to be observed than pure PFR NPs. Figure 4C further shows that the increased PL intensity of PFR NPs in the FRET probe was less affected by the added Cu^{2+} ions. When the red luminescence of QDs in the FRET probe was quenched by the added Cu^{2+} ions, the green luminescence of PFR in the nanocomposites was monitored easier and easier with the increase of the concentration of Cu^{2+} ions. Figure 4A shows that when the concentration of Cu^{2+} ions was as low as 0.16 μmol/L, the change of optical color of the PFR−QDs probe can still be observed obviously. The second reason is that under the quenching effect of Cu^{2+} ions, the optical color of the QDs is only influenced by the added Cu^{2+} ions and it changes from red to colorless. As we know that the colorlessness is not so sensitive to be observed as green. Thus, the FRET probe is more sensitive than pure QDs for visual detection of Cu^{2+} ions. On the basis of the result above, it can be concluded that the limit of detection (LOD) is 0.16 μmol/L. A comparison of this value to the LOD that Zhou *et al.* found (50 μmol/L) [43]

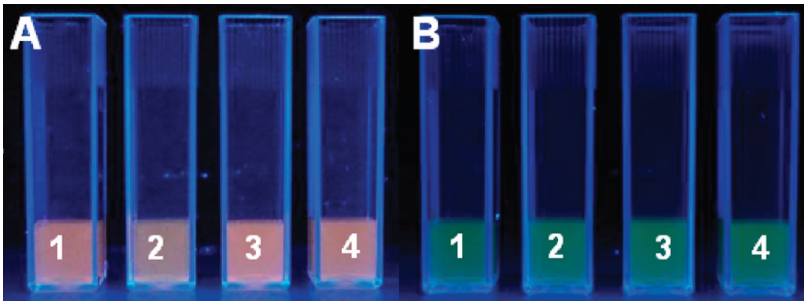

Figure 5. The optical color of 0.5 mg/mL PFR−CdTe QDs probe and different metal ions: (1) 100, 100, 100, and 10 μmol/L K^+, Zn^{2+}, Ca^{2+} and Ni^{2+}; (2) 10, 10, 10, and 5 μmol/L Cd^{2+}, Pb^{2+}, Co^{2+} and Fe^{3+}; (3) 100, 100, 10, and 10 μmol/L K^+, Zn^{2+}, Ni^{2+} and Cd^{2+}; (4) 100,10,10 and 5 μmol/L Ca^{2+}, Cd^{2+}, Mn^{2+} and Fe^{3+} in the absence (A) and in the presence (B) of Cu^{2+} ion (3.58 μmol/L) in a simulated sample.

TABLE 1. The Detection of Cu^{2+} Ions in Simulated Samples

sample	1	2	3	4
solutions with different concentrations of metal ions (μmol/L)	100 K^+, 100 Zn^{2+}, 10 Ni^{2+}, 100 Ca^{2+}, 3.58 Cu^{2+}	10 Cd^{2+}, 10 Pb^{2+}, 10 Co^{2+}, 5 Fe^{3+} 3.58 Cu^{2+}	100 K^+, 10 Ni^{2+}, 10 Cd^{2+}, 100 Zn^{2+}, 3.58 Cu^{2+}	100 Ca^{2+}, 10 Cd^{2+}, 5 Fe^{3+}, 10 Mn^{2+} 3.58 Cu^{2+}
Cu^{2+} ions found (μmol/L)	3.69	3.52	3.83	3.76
recovery (%)	103.1	98.3	106.9	105.1
RSD (%)	3.1	1.4	2.8	1.7

shows that this FRET probe provides a new way for optical visual detection of Cu^{2+} ions.

The PL spectra of the mixture of various concentrations of copper ions and 0.5 mg/mL QDs-PFR probe (Figure 4C) demonstrate that the emission of QDs in the PFR−CdTe QDs probe decreased linearly with the increase of copper ions concentration from 0.027 to 0.16 μmol/L (Figure 4C, inset). The corresponding linear regression equations is $F_0 - F = -8.26 + 11.04C$ (C, μmol/L) with a correlation coefficient of 0.9923. The LOD at a signal/noise ratio of 3 is 0.009 μmol/L, where F_0 is the PL intensity of QDs in the PFR−QDs nanocomposites in the absence of Cu^{2+}; F is the PL intensity of QDs in the FRET system in the presence of Cu^{2+}; and C is the concentration of Cu^{2+} ions added in the FRET system. Compared to the LOD obtained from the FRET probe with another method reported (3.0×10^{-7} mol/L),[46] the PFR−QDs probe presented here is also more sensitive for Cu^{2+} detection based on the PL method.

Furthermore, the UV−visible absorption spectra of PFR NPs (Figure 4D, curve a), CdTe QDs (Figure 4D, curve b) and copper ions (Figure 4D, curve c) were recorded. As shown above, there is a noticeable absorption peak at about 610 nm for PFR NPs. The absorption peak for 4.1 nm CdTe QDs is at about 400 nm and there is a distinct absorption peak at about 700 nm for copper ions (Figure 4D, curve c). However, when the concentration of the CdTe QDs or copper ions is lower than 10 μmol/L, it is difficult to observe their absorption peak through a UV−visible-NIR spectrophotometer. The addition of 0.027−0.16 μmol/L copper ions only brought a little of decrease of the absorption intensity of the PFR−QDs probe (Figure 4E). The result also demonstrates that there was some interaction between Cu^{2+} ions and the PFR−QDs probe.

To assess the potential applicability of the prepared probe, the simulated sample is often carried out in sample detection.[25,49] Hence, the applicability of the PFR−QDs FRET probe was tested in the simulated samples containing other environmentally relevant metal ions in 0.5 mL of drinkable water (obtained from Hefei in China) in the absence (Figure 5A) and in the presence (Figure 5B) of 3.58 μmol/L Cu^{2+} ions. The noticeable fluorescence color change under UV light excitation implied that this FRET probe could meet the sensitivity as well as selectivity requirements for visual detection of Cu^{2+} in environmental water samples. Also, the simulated samples were measured by fluorescence spectrophotometer, and the results were shown in Table 1. The relative standard deviation (RSD) is an important criterion to evaluate the precision of the method. Here the RSD was obtained by repeating the experiment 6 times to measure the PL data under the same conditions. The data of the recovery and the RSD found in Table 1 indicate that the method is reliable for Cu^{2+} ions detection. From Table 1 it also can be seen that the values measured by this proposed FRET probe are in good agreement with the known values for the concentration of Cu^{2+} ions in the simulated sample.

CONCLUSION

We developed a new kind of PFR−QDs FRET probe by taking advantage of their excellent sensitivity and their optical color change induced by Cu^{2+} ions so that visual detection of Cu^{2+} ions can be realized. This new probe has several advantages for Cu^{2+} ions detection. First, the probe is easily prepared and the method does not need specialized equipments or reagents. Second, this probe can detect Cu^{2+} ions at room temperature

by naked eyes within 1 min. Finally, this method exhibits excellent sensitivity for Cu^{2+} ions over other metal ions. These advantages substantially make this probe promising to be useful in the future development of other nanocomposites for Cu^{2+} ions monitoring in environment.

MATERIALS AND METHODS

All reagents are of analytical grade and used without further purification.

Chemicals. $CdCl_2 \cdot 2.5H_2O$, Te powder (Guoyao Chemicals Co., Shanghai, China), and $NaBH_4$ (Fuchen Chemicals Co., Tianjin, China) were used to prepare CdTe QDs. Mereaptoactetic acid (MA) (Sigma) was used as the capping agent. Phenol and HMT (Guoyao Chemicals Co., Shanghai, China) were used to synthesize PFR nanoparticles. Poly(sodium 4-styrene-sulfonate) (PSS, $Mw = 70000$) and polyethylenimine (PEI, branched, $Mw = 25000$, purchased from Aldrich) were used to modify the PFR NPs. The cross-linking reagent 1-ethyl-3-(3-dimethly aminopropyl) carbodiimide (EDAC) and *N*-hydroxysuccinimide (NHS) were purchased from Sigma. 4-Morpholineethanesulfonic acid hydrate (MES) (purchased from Sigma) and Phosphate Buffer Solution (PBS) (Sangon Biotech Co., Shanghai, China) were used to prepare the buffer solution. Aqueous solutions of Fe^{3+}, K^+, Na^+, Ca^{2+}, Cd^{2+}, Pb^{2+}, Mn^{2+}, Co^{2+}, Ni^{2+}, Cu^{2+}, and Zn^{2+} were prepared from $FeCl_3 \cdot 6H_2O$, KNO_3, NaCl, $Ca(NO_3)_2 \cdot 4H_2O$, $CdCl_2 \cdot 2.5H_2O$, $Pb(NO_3)_2$, $MnCl_2 \cdot 4H_2O$, $CoCl_2 \cdot 6H_2O$, $NiCl_2 \cdot 6H_2O$, $CuCl_2 \cdot 2H_2O$, and $Zn(NO_3)_2 \cdot 7H_2O$, respectively.

Synthesis of CdTe QDs. The MA−CdTe QDs were synthesized according to previous literature reported[47] with slight change. Briefly, 0.25 mmol of $CdCl_2$ and 0.625 mmol of MA were dissolved in 100 mL of N_2-saturated deionized water in a 150 mL three-neck flask and the pH was adjusted to 9.0 with a 0.1 mol/L aqueous NaOH solution. A certain amount of NaHTe solution prepared by reacting Te powder with $NaBH_4$[50] was quickly injected into the reaction solution. The molar ratio of Cd^{2+}/MA/HTe^- was fixed at 1:2.4:0.5. The solution was heated at 90 °C for refluxion under a nitrogen atmosphere. The emission wavelength of the CdTe QDs could be tuned by changing the refluxing time.

Synthesis of Functional PFR Nanoparticles. PFR NPs were synthesized according to the method we have reported.[19] The as-prepared PFR NPs were modified according to the ref 51 for a polymer coating with slight change. In brief, 1 mL aliquots of these containing 10 mg PFR NPs were put into 5 mL microcentrifuge tubes. Then, 1 mL of 10 mmol/L NaCl and 2 mL of 10 mg/mL PEI stock solution, which was prepared by dissolving an appropriate amount of PEI in 10 mmol/L NaCl solution, were mixed with PFR NPs in the microcentrifuge tubes simultaneously, and the mixture was vortexed for 2 min. After 30 min adsorption time in a dark place, the excess polymer in the supernatant fraction was removed by centrifugation (14000 rpm, 8 min), and the polymer coating PFR nanocomposites were redispersed in 1 mL of DI water for further studies. The synthesis of the PSS coating PFR followed a procedure identical to the one described above for the synthesis of the PEI coating PFR with the exception of the same amount of PSS being used. Then the third polymer was coated by repeated absorbance of PEI onto the surface of the PSS-coated PFR nanocomposites.

Preparation of the PFR-CdTe QDs Nanocomposites. Different concentrations of CdTe QDs and appropriate amount polymer coated PFR NPs were mixed and dissolved in 5 mL of water. The pH was adjusted to 5.0 with 0.1 mol/L MES buffer solution. Then 0.1 mmol of EDAC and 0.2 mmol of NHS were added and the mixture was vortexed slowly for 3 h. Excess PFR, CdTe QDs, EDAC, and NHS were removed by several repeated centrifugation separation/wash/redispersion cycles. And the CdTe QDs-conjugated PFR nanocomposties were dispersed in 10 mL of water stored at room temperature.

Response to a Series of Selected Metal Ions. A 50 μL portion of the as-synthesized PFR−QDs nanocomposites and a serial of selected metal ions (1 μmol/L) were mixed in 1.5 mL microcentrifuge tubes, respectively. Then, the mixtures were diluted by 0.01 mol/L PBS (pH = 7) solution to give a total volume of 1 mL. The optical color change was observed under excitation at UV lamp (excitation wavelength at 365 nm) within 1 min, and the spectra were measured by a fluorescence spectrophotometer (F-7000, Hitachi) excited at 340 nm.

Detection of Cu^{2+} Ions. The experiment of detection of Cu^{2+} ions with the as-synthesized PFR-CdTe QDs followed a procedure identical as the one described above for a series of selected metal ions. A 50 μL portion of the as-synthesized PFR−QDs nanocomposites and 0.08, 0.16, 0.25, 0.43, 2.87, and 5.36 μmol/L Cu^{2+} ions were mixed in 1.5 mL microcentrifuge tubes, respectively. Then, the mixtures were diluted by 0.01 mol/L PBS (pH = 7) solution to give a total volume of 1 mL. The optical color change was observed under excitation at UV lamp (excitation wavelength at 365 nm) within 1 min.

Optical Visual Assay for Cu^{2+} Ions in Simulated Sample. Different concentrations of metal ions were mixed with 0.5 mL of drinking-water (obtained from Hefei in China) for the preparation of simulated samples. A 50 μL portion of the as-synthesized PFR−QDs nanocomposites were added into the above sample in 1.5 mL microcentrifuge tubes. Then, the PBS solutions were added to give a total volume of 1 mL. The procedure of optical detection followed the one described above for the Cu^{2+} ions detection.

Characterization of the FRET Probe Composed of PFR and CdTe QDs. Surface charges (zeta potentials) were measured on a Nano-ZS Zetasizer (Malvern Instruments, UK) equipped with a 4.0 mW internal laser. The formation of carbonyl groups between PFR and CdTe QDs was characterized by FTIR spectra and XPS spectra. FTIR spectra were measured on a Bruker Vector-22 FTIR spectrometer from 4000 to 400 cm^{-1} at room temperature. X-ray photoelectron spectroscopy (XPS) analysis was measured on electron spectrometer (ESCALAB 250, Thermo-VG Scientific). The morphologies were observed by transmission electron microscope (TEM, JEOL-2010). High-resolution transmission electron microscope (HRTEM) images were performed on a JEOL-2010 transmission electron microscope operated at an acceleration voltage of 200 kV. The elemental composition was analyzed by inductive coupled plasma emission spectrometer (ICP, SCIEX ELAN DRC-e). Fluorescence microscopy images were observed by the excitation of UV light at 365 nm. The fluorescence spectra of PFR, CdTe, and the PFR−QDs probe were investigated by a fluorescence spectrophotometer (F-7000, Hitachi) excited at 340 nm.

Acknowledgment. This work is supported by the National Basic Research Program of China (2010CB934700), the National Natural Science Foundation of China (Nos. 91022032, 50732006), International Science & Technology Cooperation Program of China (2010DFA41170), the Principle Investigator Award by the National Synchrotron Radiation Laboratory at the University of Science and Technology of China, and the Natural Science Foundation of the Educational Department of Anhui Province (KJ2009B265Z).

Supporting Information Available: Hydrodynamic diameters, zeta potentials, FTIR spectrum, and XPS data details. This material is available free of charge *via* the Internet at http://pubs.acs.org.

REFERENCES AND NOTES

1. Ho, H. A.; Dore, K.; Boissinot, M.; Bergeron, M. G.; Tanguay, R. M.; Boudreau, D.; Leclerc, M. Direct Molecular Detection of Nucleic Acids by Fluorescence Signal Amplification. *J. Am. Chem. Soc.* **2005,** *127*, 12673–12676.
2. Kajihara, D.; Abe, R.; Iijima, I.; Komiyama, C.; Sisido, M.; Hohsaka, T. FRET Analysis of Protein Conformational

Change through Position-Specific Incorporation of Fluorescent Amino Acids. *Nat. Methods*. **2006,** *3*, 923–929.
3. Iqbal, A.; Wang, L.; Thompson, K. C.; Lilley, D. M. J.; Norman, D. G. The Structure of Cyanine 5 Terminally Attached to Double-Stranded DNA: Implications for FRET Studies. *Biochemistry* **2008,** *47*, 7857–7862.
4. Yea, K. H.; Lee, S.; Choo, J.; Oh, C. H. Fast and Sensitive Analysis of DNA Hybridization in a PDMS Micro-fluidic Channel Using Fluorescence Resonance Energy Transfer. *Chem. Commun.* **2006,** 1509–1511.
5. Eichelbaum, M.; Rademann, K. Plasmonic Enhancement or Energy Transfer? On the Luminescence of Gold-, Silver-, and Lanthanide-Doped Silicate Glasses and Its Potential for Light-Emitting Devices. *Adv. Funct. Mater.* **2009,** *19*, 2045–2052.
6. Reil, F.; Hohenester, U.; Krenn, J. R.; Leitner, A. Forster-Type Resonant Energy Transfer Influenced by Metal Nanoparticles. *Nano Lett.* **2008,** *8*, 4128–4133.
7. Lu, H.; Schops, O.; Woggon, U.; Niemeyer, C. M. Self-Assembled Donor Comprising Quantum Dots and Fluorescent Proteins for Long-Range Fluorescence Resonance Energy Transfer. *J. Am. Chem. Soc.* **2008,** *130*, 4815–4827.
8. Jiang, G. X.; Susha, A. S.; Lutich, A. A.; Stefani, F. D.; Feldmann, J.; Rogach, A. L. Cascaded FRET in Conjugated Polymer/Quantum Dot/Dye-Labeled DNA Complexes for DNA Hybridization Detection. *ACS Nano* **2009,** *3*, 4127–4131.
9. Boeneman, K.; Delehanty, J. B.; Susumu, K.; Stewart, M. H.; Medintz, I. L. Intracellular Bioconjugation of Targeted Proteins with Semiconductor Quantum Dots. *J. Am. Chem. Soc.* **2010,** *132*, 5975–5977.
10. Hildebrandt, N.; Charbonniere, L. J.; Beck, M.; Ziessel, R. F.; Lohmannsroben, H. G. Quantum Dots as Efficient Energy Acceptors in a Time-Resolved Fluoroimmunoassay. *Angew. Chem., Int. Ed.* **2005,** *44*, 7612–7615.
11. Goldman, E. R.; Medintz, I. L.; Whitley, J. L.; Hayhurst, A.; Clapp, A. R.; Uyeda, H. T.; Deschamps, J. R.; Lassman, M. E.; Mattoussi, H. A Hybrid Quantum Dot-Antibody Fragment Fluorescence Resonance Energy Transfer-Based TNT Sensor. *J. Am. Chem. Soc.* **2005,** *127*, 6744–6751.
12. Suzuki, M.; Husimi, Y.; Komatsu, H.; Suzuki, K.; Douglas, K. T. Quantum Dot FRET Biosensors That Respond to pH, to Proteolytic or Nucleolytic Cleavage, to DNA Synthesis, or to a Multiplexing Combination. *J. Am. Chem. Soc.* **2008,** *130*, 5720–5725.
13. Gill, R.; Bahshi, L.; Freeman, R.; Willner, I. Optical Detection of Glucose and Acetylcholine Esterase Inhibitors by H_2O_2 Sensitive CdSe/ZnS Quantum Dots. *Angew. Chem., Int. Ed.* **2008,** *47*, 1676–1679.
14. Freeman, R.; Gill, R.; Shweky, I.; Kotler, M.; Banin, U.; Willner, I. Biosensing and Probing of Intracellular Metabolic Pathways by NADH-Sensitive Quantum Dots. *Angew. Chem., Int. Ed.* **2009,** *48*, 309–313.
15. Oh, E.; Hong, M. Y.; Lee, D.; Nam, S. H.; Yoon, H. C.; Kim, H. S. Inhibition Assay of Biomolecules Based on Fluorescence Resonance Energy Transfer (FRET) between Quantum Dots and Gold Nanoparticles. *J. Am. Chem. Soc.* **2005,** *127*, 3270–3271.
16. Pons, T.; Medintz, I. L.; Sapsford, K. E.; Higashiya, S.; Grimes, A. F.; English, D. S.; Mattoussi, H. On the Quenching of Semiconductor Quantum Dot Photoluminescence by Proximal Gold Nanoparticles. *Nano Lett.* **2007,** *7*, 3157–3164.
17. Kim, Y. P.; Oh, Y. H.; Oh, E.; Ko, S.; Han, M. K.; Kim, H. S. Energy Transfer-Based Multiplexed Assay of Proteases by Using Gold Nanoparticle and Quantum Dot Conjugates on a Surface. *Anal. Chem.* **2008,** *80*, 4634–4641.
18. Haldar, K. K.; Sen, T.; Patra, A. Metal Conjugated Semiconductor Hybrid Nanoparticle-Based Fluorescence Resonance Energy Transfer. *J. Phys. Chem. C* **2010,** *114*, 4869–4874.
19. Guo, S. R.; Gong, J. Y.; Jiang, P.; Wu, M.; Lu, Y.; Yu, S. H. Biocompatible, Luminescent Silver@phenol Formaldehyde Resin Core/Shell Nanospheres: Large-Scale Synthesis and Application for *in Vivo* Bioimaging. *Adv. Funct. Mater.* **2008,** *18*, 872–879.
20. Barnham, K. J.; Bush, A. I. Metals in Alzheimer's and Parkinson's Diseases. *Curr. Opin. Chem. Biol.* **2008,** *12*, 222–228.
21. Crichton, R. R.; Dexter, D. T.; Ward, R. J. Metal Based Neurodegenerative Diseases—From Molecular Mechanisms to Therapeutic Strategies. *Coord. Chem. Rev.* **2008,** *252*, 1189–1199.
22. Taki, M.; Iyoshi, S.; Ojida, A.; Hamachi, I.; Yamamoto, Y. Development of Highly Sensitive Fluorescent Probes for Detection of Intracellular Copper(I) in Living Systems. *J. Am. Chem. Soc.* **2010,** *132*, 5938–5939.
23. Lan, G. Y.; Huang, C. C.; Chang, H. T. Silver Nanoclusters as Fluorescent Probes for Selective and Sensitive Detection of Copper Ions. *Chem. Commun.* **2010,** *46*, 1257–1259.
24. Lin, W. Y.; Long, L. L.; Chen, B. B.; Tan, W.; Gao, W. S. Fluorescence Turn-On Detection of Cu^{2+} in Water Samples and Living Cells Based on the Unprecedented Copper-Mediated Dihydrorosamine Oxidation Reaction. *Chem. Commun.* **2010,** *46*, 1311–1313.
25. Chan, Y. H.; Chen, J. X.; Liu, Q. S.; Wark, S. E.; Son, D. H.; Batteas, J. D. Ultrasensitive Copper(II) Detection Using Plasmon-Enhanced and Photo-Brightened Luminescence of CdSe Quantum Dots. *Anal. Chem.* **2010,** *82*, 3671–3678.
26. Xiang, G. Q.; Zhang, Y. M.; Jiang, X. M.; He, L. J.; Fan, L.; Zhao, W. J. Determination of Trace Copper in Food Samples by Flame Atomic Absorption Spectrometry after Solid Phase Extraction on Modified Soybean Hull. *J. Hazard. Mater.* **2010,** *179*, 521–525.
27. Wu, J. F.; Boyle, E. A. Low Blank Preconcentration Technique for the Determination of Lead, Copper, and Cadmium in Small-Volume Seawater Samples by Isotope Dilution ICPMS. *Anal. Chem.* **1997,** *69*, 2464–2470.
28. Lee, S.; Choi, I.; Hong, S.; Yang, Y. I.; Lee, J.; Kang, T.; Yi, J. Highly Selective Detection of Cu^{2+} Utilizing Specific Binding Between Cu-Demetallated Superoxide Dismutase 1 and the Cu^{2+} Ion *via* Surface Plasmon Resonance Spectroscopy. *Chem. Commun.* **2009,** 6171–6173.
29. Zheng, Y. J.; Gattas-Asfura, K. M.; Konka, V.; Leblanc, R. M. A Dansylated Peptide for the Selective Detection of Copper Ions. *Chem. Commun.* **2002,** 2350–2351.
30. Lin, M.; Cho, M. S.; Choe, W. S.; Lee, Y. Electrochemical Analysis of Copper Ion Using a Gly−Gly−His Tripeptide Modified Poly(3-thiopheneacetic acid) Biosensor. *Biosens. Bioelectron.* **2009,** *25*, 28–33.
31. Etienne, M.; Bessiere, J.; Walcarius, A. Voltammetric Detection of Copper(II) at a Carbon Paste Electrode Containing an Organically Modified Silica. *Sens. Actuators, B* **2001,** *76*, 531–538.
32. Kim, S.; Park, J. W.; Kim, D.; Lee, I. H.; Jon, S. Bioinspired Colorimetric Detection of Calcium(II) Ions in Serum Using Calsequestrin-Functionalized Gold Nanoparticles. *Angew. Chem., Int. Ed.* **2009,** *48*, 4138–4141.
33. Prabhakaran, D.; Ma, Y. H.; Nanjo, H.; Matsunaga, H. Naked-Eye Cadmium Sensor: Using Chromoionophore Arrays of Langmuir−Blodgett Molecular Assemblies. *Anal. Chem.* **2007,** *79*, 4056–4065.
34. Huang, K. W.; Yu, C. J.; Tseng, W. L. Sensitivity Enhancement in the Colorimetric Detection of Lead(II) Ion Using Gallic Acid-Capped Gold Nanoparticles: Improving Size Distribution and Minimizing Interparticle Repulsion. *Biosens. Bioelectron.* **2010,** *25*, 984–989.
35. Ranyuk, E.; Douaihy, C. M.; Bessmertnykh, A.; Denat, F.; Averin, A.; Beletskaya, I.; Guilard, R. Diaminoanthraquinone-Linked Polyazamacrocycles: Efficient and Simple Colorimetric Sensor for Lead Ion in Aqueous Solution. *Org. Lett.* **2009,** *11*, 987–990.
36. Lee, J. S.; Han, M. S.; Mirkin, C. A. Colorimetric Detection of Mercuric Ion (Hg^{2+}) in Aqueous Media Using DNA-Functionalized Gold Nanoparticles. *Angew. Chem., Int. Ed.* **2007,** *46*, 4093–4096.
37. Xue, X. J.; Wang, F.; Liu, X. G. One-Step Room Temperature, Colorimetric Detection of Mercury (Hg^{2+}) Using DNA/Nanoparticle Conjugates. *J. Am. Chem. Soc.* **2008,** *130*, 3244–3245.

38. Li, T.; Dong, S. J.; Wang, E. Label-free Colorimetric Detection of Aqueous Mercury Ion (Hg^{2+}) Using Hg^{2+}-Modulated G-Quadruplex-Based DNAzymes. *Anal. Chem.* **2009,** *81*, 2144–2149.
39. Wang, Y.; Yang, F.; Yang, X. R. Colorimetric Biosensing of Mercury(II) Ion Using Unmodified Gold Nanoparticle Probes and Thrombin-Binding Aptamer. *Biosens. Bioelectron.* **2010,** *25*, 1994–1998.
40. Coll, C.; Martinez-Manez, R.; Marcos, M. D.; Sancenon, F.; Soto, J. A Simple Approach for the Selective and Sensitive Colorimetric Detection of Anionic Surfactants in Water. *Angew. Chem., Int. Ed.* **2007,** *46*, 1675–1678.
41. Kalluri, J. R.; Arbneshi, T.; Khan, S. A.; Neely, A.; Candice, P.; Varisli, B.; Washington, M.; McAfee, S.; Robinson, B.; Banerjee, S.; *et al.* Use of Gold Nanoparticles in a Simple Colorimetric and Ultrasensitive Dynamic Light Scattering Assay: Selective Detection of Arsenic in Groundwater. *Angew. Chem., Int. Ed.* **2009,** *48*, 9668–9671.
42. Xu, W.; Xue, X. J.; Li, T. H.; Zeng, H. Q.; Liu, X. G. Ultrasensitive and Selective Colorimetric DNA Detection by Nicking Endonuclease Assisted Nanoparticle Amplification. *Angew. Chem., Int. Ed.* **2009,** *48*, 6849–6852.
43. Zhou, Y.; Wang, S. X.; Zhang, K.; Jiang, X. Y. Visual Detection of Copper(II) by Azide- and Alkyne-Functionalized Gold Nanoparticles Using Click Chemistry. *Angew. Chem., Int. Ed.* **2008,** *47*, 7454–7456.
44. Yin, B. C.; Ye, B. C.; Tan, W. H.; Wang, H.; Xie, C. C. An Allosteric Dual-DNAzyme Unimolecular Probe for Colorimetric Detection of Copper(II). *J. Am. Chem. Soc.* **2009,** *131*, 14624–14625.
45. Xu, X. Y.; Daniel, W. L.; Wei, W.; Mirkin, C. A. Colorimetric Cu^{2+} Detection Using DNA-Modified Gold-Nanoparticle Aggregates as Probes and Click Chemistry. *Small* **2010,** *6*, 623–626.
46. Zhao, Y.; Zhang, X. B.; Han, Z. X.; Qiao, L.; Li, C. Y.; Jian, L. X.; Shen, G. L.; Yu, R. Q. Highly Sensitive and Selective Colorimetric and Off−On Fluorescent Chemosensor for Cu^{2+} in Aqueous Solution and Living Cells. *Anal. Chem.* **2009,** *81*, 7022–7030.
47. Zhang, H.; Zhou, Z.; Yang, B.; Gao, M. Y. The Influence of Carboxyl Groups on the Photoluminescence of Mercaptocarboxylic Acid-Stabilized CdTe Nanoparticles. *J. Phys. Chem. B.* **2003,** *107*, 8–13.
48. Costa, L.; diMontelera, L. R.; Camino, G.; Weil, E. D.; Pearce, E. M. Structure-Charring Relationship in Phenol-Formaldehyde Type Resins. *Polym. Degrad. Stab.* **1997,** *56*, 23–35.
49. Guo, Z. Q.; Chen, W. Q.; Duan, X. M. Highly Selective Visual Detection of Cu(II) Utilizing Intramolecular Hydrogen Bond-Stabilized Merocyanine in Aqueous Buffer Solution. *Org. Lett.* **2010,** *12*, 2202–2205.
50. Zhang, H.; Wang, L. P.; Xiong, H. M.; Hu, L. H.; Yang, B.; Li, W. Hydrothermal Synthesis for High-Quality CdTe Nanocrystals. *Adv. Mater.* **2003,** *15*, 1712–1715.
51. Gole, A.; Murphy, C. J. Biotin−Streptavidin-Induced Aggregation of Gold Nanorods: Tuning Rod−Rod Orientation. *Langmuir* **2005,** *21*, 10756–10762.